Near real-time delineation, mapping and monitoring of floods in West Bengal, India due to extremely severe cyclone ‘Amphan’ using multi-mission satellite data

S. V. Shiva Prasad Sharma*, K. H. V. Durga Rao and Abhinav K. Shukla

Disaster Management Support Group, Remote Sensing Applications Area, National Remote Sensing Centre, Indian Space Research Organisation, Balanagar, Hyderabad 500 037, India

The extremely severe cyclone ‘Amphan’ made landfall on 20 May 2020 in the state of West Bengal, India causing widespread damages. The present study describes the potential use of multi-mission satellite datasets in delineating the cyclone disaster footprints and assessing the impact in near real-time. Flooding due to the cyclone was monitored and mapped continuously from 21 to 27 May 2020 using synthetic aperture radar (SAR) data of multiple satellites. It was observed that about 2.09 lakh hectares in ten districts of the state was affected by cyclone-induced inundation. East Medinipur district was the worst affected with 83,402 ha inundated during the cyclone. The inundation maps were disseminated to the disaster management authorities in near real-time for effective disaster management to aid in relief and rescue operations.

Keywords: Cyclone, near real-time monitoring, multi-mission satellite data, flood impact assessment.

CYCLONES are the most frequent natural disasters affecting the large coastline of India. According to the World Meteorological Organization[1], tropical cyclones are traditionally used to denote tropical weather systems globally. These cyclones are usually associated with high-velocity winds, intense rainfall and storm surges[2]. Among 7516 km of the Indian coastline, about 5400 km lies along the mainland exposing major cities like Chennai, Kolkata, Mumbai, etc. to cyclones and storm surges.

Cyclones, characterized as the major meteorological hazards, associated with high-velocity winds and rainfall cause damage to crops, industrial and residential infrastructure, communication networks, etc.

The Intergovernmental Panel for Climate Change (IPCC) indicates ‘rise in cyclone hazards and mortality in weakest governance capacities since 1980’. Even though cyclones cannot be stopped, but *a priori* information on forewarning or prediction of a cyclone plays a prominent role towards evacuation of people and minimizing loss of lives. Accurate numerical weather predictions are an important prerequisite for cyclone landfall prediction and forewarning, as they help deal with the various phases of cyclone-induced disasters. About 88 cyclones were observed to form on an average each year during 1968–2010 across the world[3,4]. During the last decade, India has suffered severe damages to property and infrastructure due to cyclones Phailin (2013), Hudhud (2014), Vardah (2016) and Titl (2018), etc.

The damage caused by cyclones cannot be avoided, but they can be minimized using proper disaster management approaches. Satellite remote sensing coupled with Geographic Information System can be useful in addressing various phases of cyclone disaster management[5–7]. Temporal remote sensing data are traditionally used to assess changes in infrastructure environmental conditions at regular intervals. The revisit capability of satellites at regular intervals is used advantageously to map, monitor and manage disasters efficiently and can also aid in understanding the pattern of flooding, such as progression and recession phases of the flood cycle.

The availability of high-resolution satellite datasets at frequent intervals of the order of sub-metre spatial resolution will be an invaluable addition to assess damage to infrastructure and urban settlements. Many studies have been conducted across the globe related to cyclone disaster management phases using remote sensing and GIS[5,6,8].

In the present study, we assess the impact of cyclone Amphan post landfall in West Bengal, India, in near real-time using synthetic aperture radar (SAR) data, and damage to infrastructure using high-resolution (HR) satellite data acquired from multiple space missions across the globe.

Study area

The study area lies between 21°25′–27°13′N and 85°50′–89°50′E with a total geographical area of 88,752 sq. km.

*For correspondence. (e-mail: sharma12644@gmail.com)

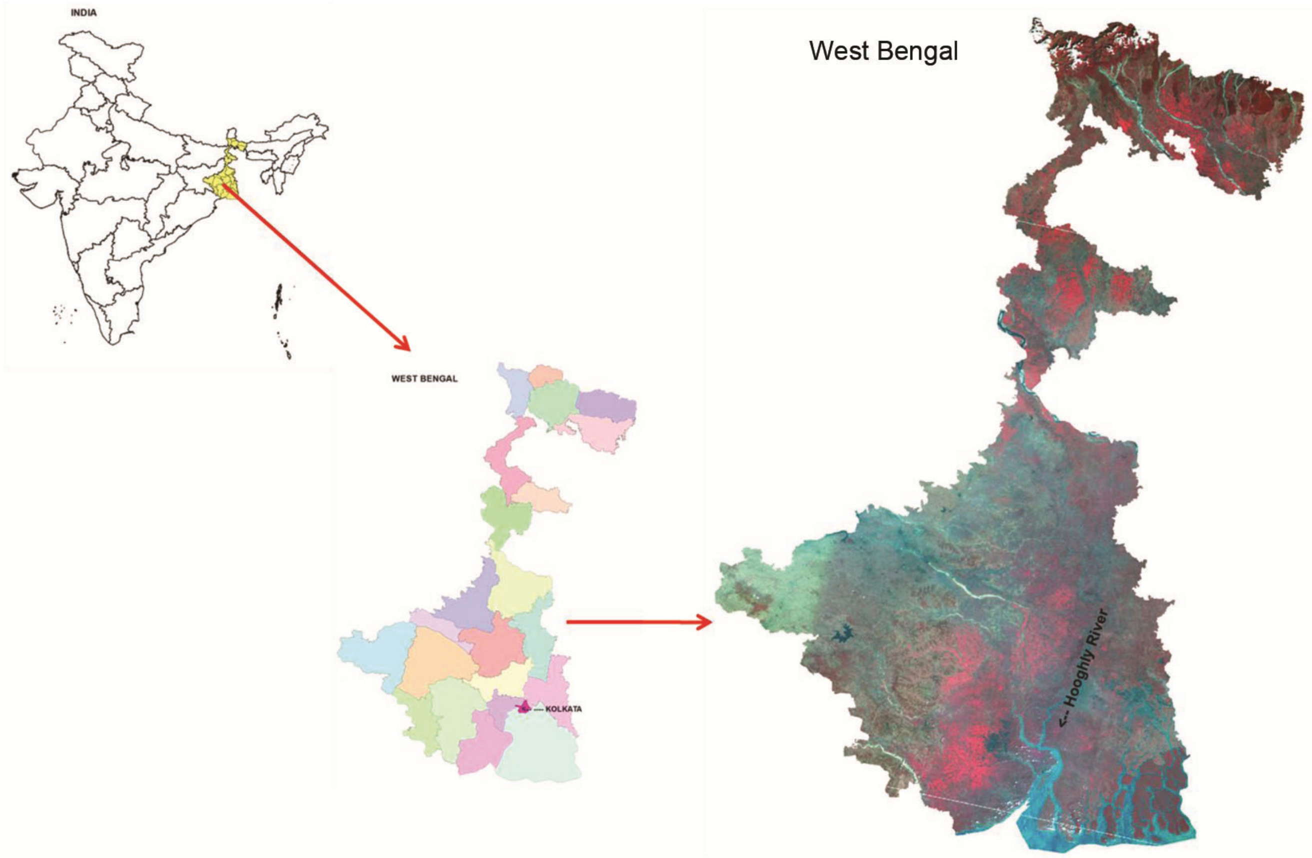

Figure 1. Location map of the study area; West Bengal, India (source: NRSC/ISRO).

The state is located in eastern India and is the gateway to the North East states. The picturesque Himalaya is to the north of the west Bengal, while Bay of Bengal is in the south and southeast. The state shares its international borders with Bangladesh in the east. According to Census of India, 2011, the total population of West Bengal is 91,347,736. The state is divided into 19 administrative districts. The only urbanized district Kolkata, which is the third largest urban conglomeration in India and the seventh largest city in the country (Figure 1).

According to the West Bengal Disaster Management Department and Civil Authority (WBDMD; http://wbdmd.gov.in/pages/cyclone.aspx), the state experienced 54 cyclones between 1891 and 2019, of which 30 were severe cyclonic storms (http://www.rmcchennaieatlas.tn.nic.in/Plotting_ByParam.aspx). During May 2009, cyclone Aila crossed West Bengal near Sagar Islands as a severe cyclonic storm killing more than 137 people and incurred cattle loss of 50,000. The recent extremely severe cyclone Amphan is the second most devastating storm after the historic 1737 super cyclone which claimed more than 300,000 lives.

The state is bestowed with diverse landforms such as the Himalayan region in the north, the Terai region at the base of Himalayan region, the North Bengal Plains extending from the south of the Terai region and continuing to the Ganges river followed by Rarh region intervening between the Vajjabhumi and Ganges delta. The Rarh region is about 50–100 m amsl. The state has a small coastal plain bordering the Medinipur districts, and North and South 24 Paraganas. The largest mangrove area of Sundarbans which is a UNESCO world heritage site, borders the state to the south adjoining the Bay of Bengal.

Extremely severe cyclone Amphan monitoring

On 13 May 2020, a low-pressure area was formed over southeastern Bay of Bengal to the southeast of Vishakhapatnam, Andhra Pradesh, India. Over the next two days, the system gradually developed into a depression, and further strengthened and moved to the north in a few hours to form a cyclonic storm named Amphan. During 17 May 2020, it is intensified into an extremely severe cyclonic storm. During 18 May 2020, Amphan reached its peak intensity and was labelled a super cyclonic storm gathering wind speeds in excess of 240 km/h. In the following days, the cyclone weakened due to the effects of dry air and wind shear and on 20 May 2020 between 1000 and 1100 UTC, it made landfall as an

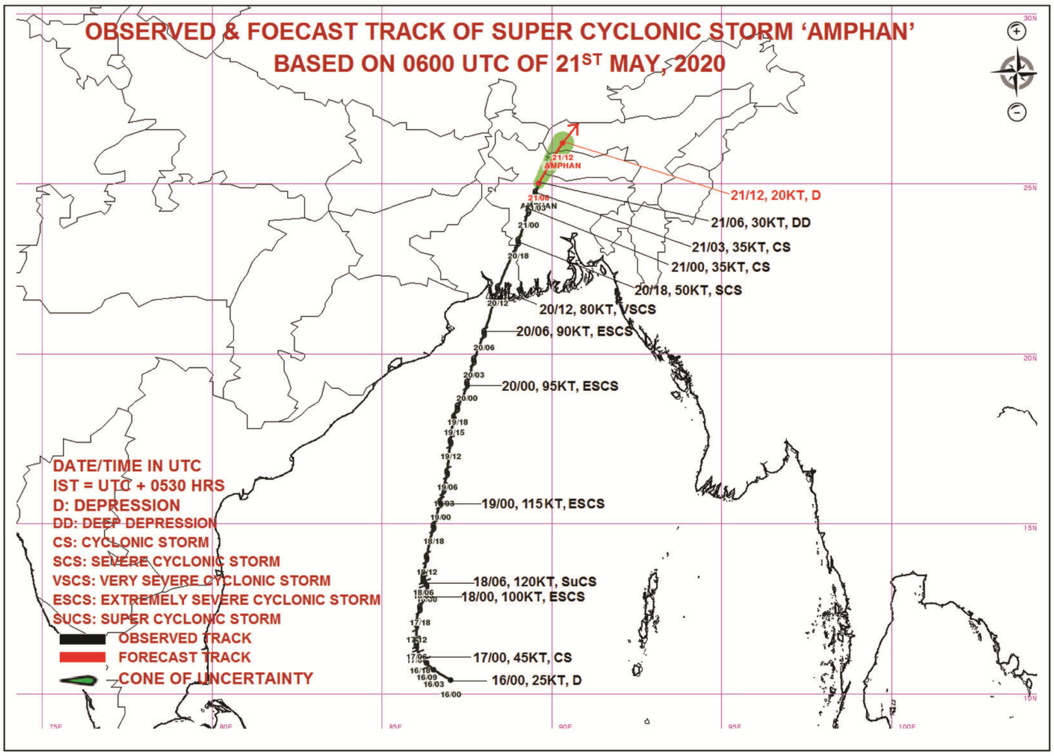

Figure 2. Track of cyclone Amphan (source: India Meteorological Department).

extremely severe cyclonic storm near Bakkhali, West Bengal. Figure 2 shows the track of cyclone Amphan.

Materials and methods

In the present study, Indian Remote Sensing Satellite Resourcesat-2 advanced wide imaging field sensor (AWiFS) data (spatial resolution of 56 m) collected on 1 March 2020, has been geometrically co-registered with the base map of the study area. Subsequently, the river banks were delineated using 'on-screen digitization' technique and overlaid on the water bodies derived from the land use/cover data of 2017–18 generated under ISRO-Natural Resources Census project. The post-landfall imageries acquired were further geo-referenced with the Resourcesat-2 AWiFS image of 1 March 2020 using Erdas Imagine COT package. The base layers consisting of administrative boundaries such as state, district, block and village at 1 : 50,000 scale provided by the State Remote Sensing Application Centre (WB-RSAC), Government of West Bengal, have been used in the study. Sentinel-2 SAR data of 9 May 2020 (https://peps.cnes.fr/rocket/) and the HR satellite imageries received under the International Charter for Space and Major Disasters (ICSMD) have been used for assessing infrastructure damage and water accumulation in the low-lying areas.

The study area of West Bengal was observed to be persistently cloudy during the study period of 20–27 May 2020. As a result, microwave data were preferred for mapping, monitoring and analysing the inundation due to cyclone-induced heavy rainfall. The SAR data due to their all-weather capability can penetrate clouds and enable delineating inundation due to predominant specular reflection from waterlogged areas on the ground.

Microwave images provided under ICSMD include datasets from satellites (Table 1).

Sentinel Asia

The Sentinel Asia (SA) initiative is a collaboration between various regional space agencies and disaster management authorities utilizing the aerospace and Web-GIS technologies to address disaster management in the Asia-Pacific region. SA was established in 2006 with Japan Aerospace Exploration Agency (JAXA) being the lead agency[9].

Space agencies under this forum contribute satellite data to the member countries upon activation of emergency observation request (EOR) to SA. There are several space agencies, namely JAXA, Indian Space Research Organization (ISRO), National Applied Research laboratories (NARL, Taiwan), Geo-Informatics and Space Technology Development Agency (GISTDA, Thailand), Korea Aerospace Research Institute (KARI, South Korea), etc. that serve as the data provider node (DPN), whose primary mandate is to supply satellite

Table 1. List of satellites and sensors utilized for inundation mapping

Satellite/sensor	Beam/mode	Date of pass	Polarization	Incidence angle (degree)	Resolution (m)
RADARSAT-2 SAR	Scan SAR wide/ascending	21 May 2020	HH	20–49	50
ALOS 2 PALSAR	Stripmap	21 May2020	HH	20–40	6
Sentinel-1 SAR	IWS/ascending	22 May 2020	VH	25	10
Terra SAR X	Scan SAR/ascending	24 May 2020	HH	20–45	18.5
RADARSAT-2 SAR	Ultra fine/ascending	24 May 2020	HH	20–49	3
		25 May 2020			3
COSI SAR	WS/ascending	27 May 2020	HH	20–45	20

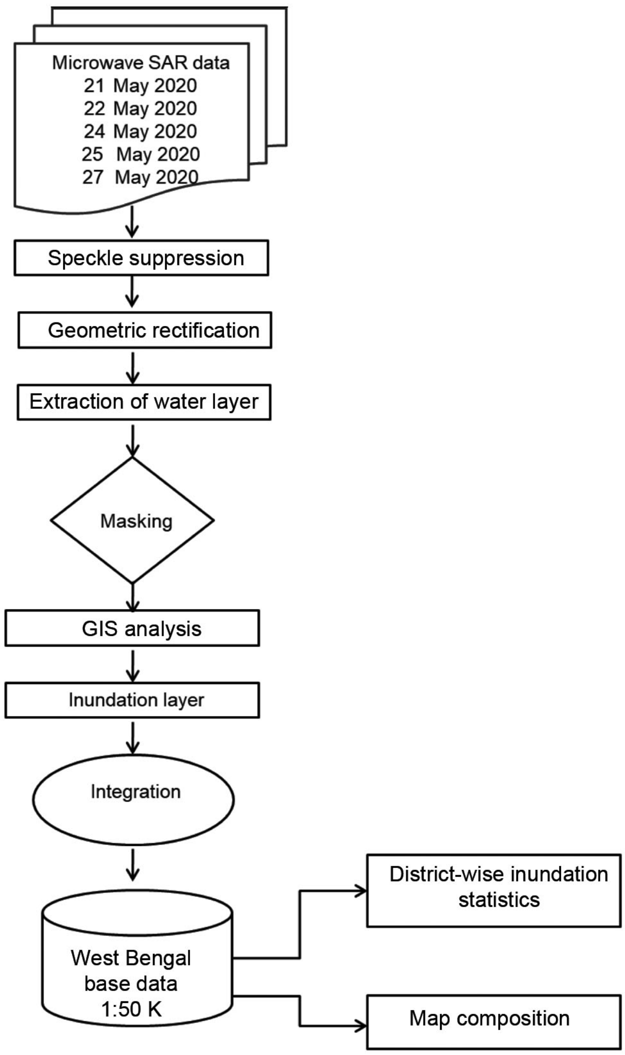

Figure 3. Delineation of inundation layer from synthetic aperture radar (SAR) data analysis.

data on request basis with other agencies, namely Geo-Informatics Centre – Asian Institute of Technology (GIC-AIT, Thailand), International Water Management Institute (IWMI, Sri Lanka), Asian Disaster Reduction Centre (ADRC, Kobo, Japan), etc. mandated to be DANs, who contribute value added products (VAP) for disaster relief and rescue measures.

Under this forum ISRO, a member organization, has activated the EOR for cyclone Amphan and received ALOS-2 PALSAR data from JAXA (Table 1).

International charter for space and major disasters

The International charter is a unified system and consensus between space agencies to support space-based data towards disaster relief and rescue. It is a unified system for data acquisition and distribution to the affected natural or man-made disasters via authorized users (AUs)[10]. It was established in 2000 and ISRO has been a member since 2001. ISRO has activated charter for HR optical and SAR data for supporting cyclone Amphan disaster mapping, monitoring and response.

Methodology

Satellite data analysis

The microwave data from SAR satellite missions were downloaded and processed for removing the inherent speckle noise associated with SAR imagery; leaving speckle unfiltered would leave large variations of radar response in homogeneous areas of the imagery leading to misclassification. The speckle filtering was done using Speckle Suppression Module of ERDAS Imagine Software. The raw images were filtered using a 3×3 matrix of Gamma maximum a posteriori (Gamma MAP) because of its superior speckle smoothing capacity[11]. To suppress spike noise, which gamma MAP leaves unfiltered on the basis of detecting it as point target, the images were subsequently filtered using a 3×3 moving-window Median filter. While gamma MAP filter preserved the land cover features and objects and exhibited better contrast between land and water, the median filter preserved the step edges while maintaining homogeneity of the image. Hence, the gamma MAP filter of 3×3 window is adopted for speckle suppression in the study. The filtered images were further geometrically co-registered with the master referenced image to attain the positional accuracy and to assign the projection system in synchronisation with the

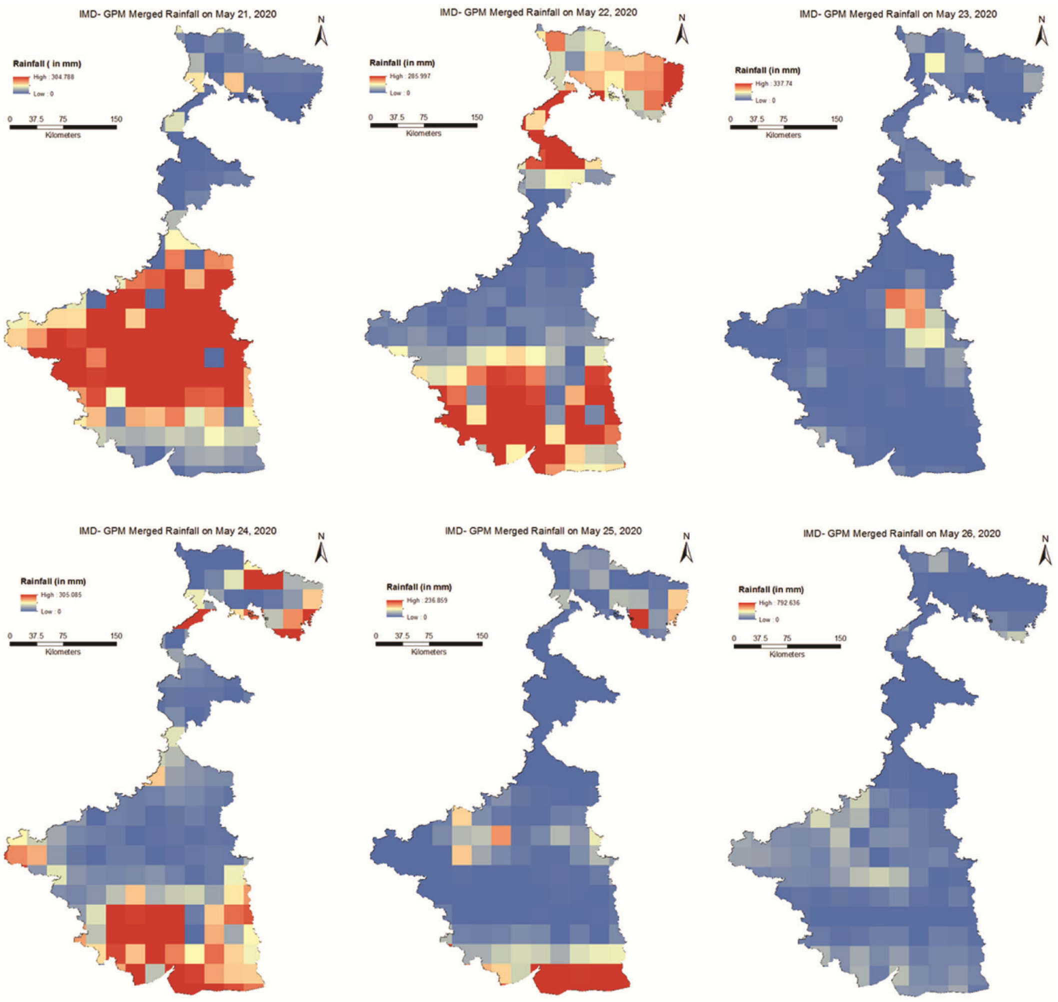

Figure 4. Rainfall observed in West Bengal during 21–26 May 2020 (source: IMD-GPM merged rainfall).

base data. In order to differentiate between flooded and non-flooded pixels, thresholding technique was adopted[12]. Thresholding segregates the values of the pixels falling above the threshold value as non-flooded and those falling within the threshold as flooded areas. In the case of RADARSAT SAR and COSI SAR X-band data after converting to backscatter images, the flooded areas are classified with threshold values lying between –8 to –12 dB in the case of horizontal transmit, horizontal receive (HH) polarization and between –15 and –24 dB in the case of horizontal transmit and vertical receive (HV) and vertical transmit and horizontal receive (VH) polarization channels, whereas in the case of Terra SAR-X (HH) and Sentinel-1 SAR C (VH), the backscatter images were able to delineate water between –24 and –30 dB. In the case of ALOS-2 PALSAR L-band data, the water pixels were classified in the range –30 to –40 dB. The application of threshold values for all the images may incur either overestimation or underestimation of water classification depending on the local conditions. Hence the variable incidence angle threshold technique was used to extract water from the images[13]. The microwave images of SAR in X, C and L-band frequencies were classified using variable incidence thresholding technique to classify the water pixels and used for inundation mapping. The SAR data of C- and X-bands were effective in delineating the inundation in open surfaces/channels (non-obstructed areas) and L-band data were useful to identify inundation in marshy lands/wastelands and in agricultural fields because of their greater penetration and longer wavelength. The image obtained after threshold was overlaid with the permanent water bodies mask, hill mask and hill shadows mask to map inundation areas due to cyclone-induced flooding. Figure 3 shows the detailed workflow of SAR data analysis to derive the inundation layer.

Further, the derived water layer was checked for discrete pixels which were removed using neighbourhood analysis. This operation removes stray pixels. It is well known that flood is a contiguous phenomenon and hence this operation ensures that stray pixels are removed. The water layer obtained after masking was further edited to arrive at a single bit thematic flood layer in which

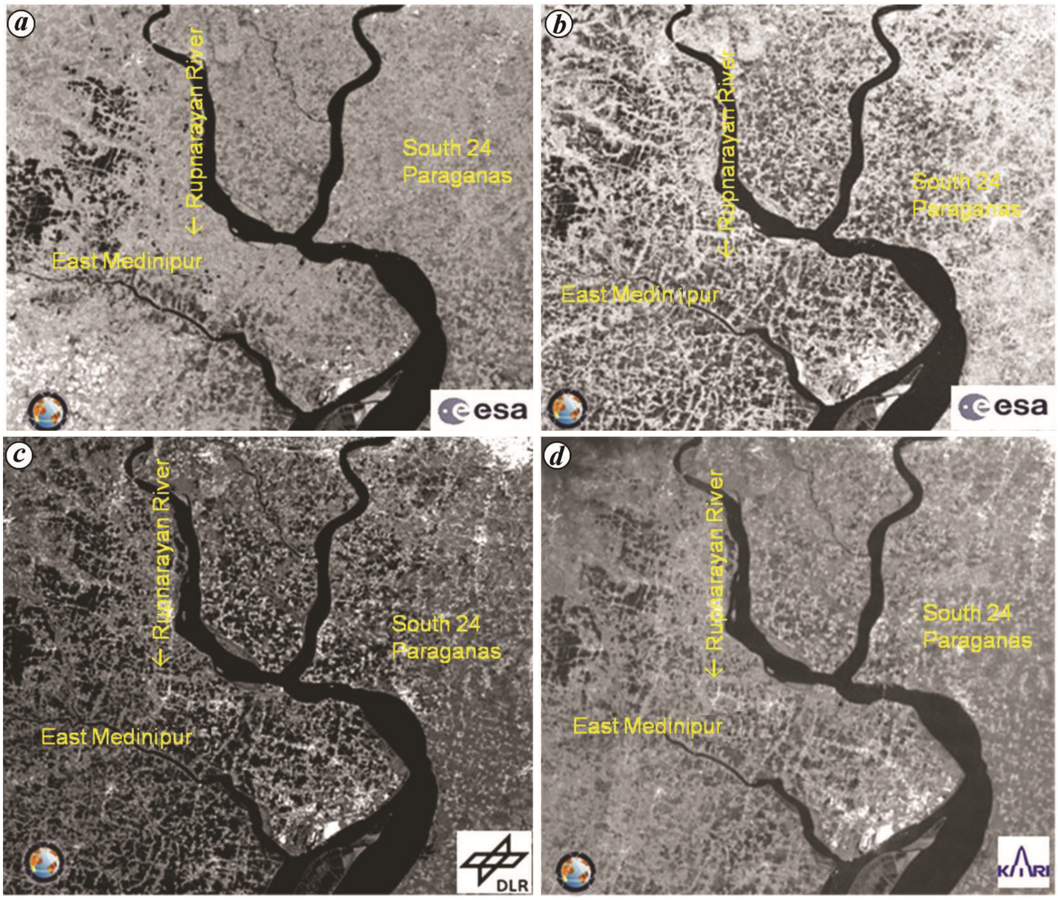

Figure 5. Four sample images acquired over parts of West Bengal during 22–27 May 2020 under the International Charter 5. ***a***, Sentinel-1 SAR image of 25 April 2020, Copernicus Sentinel data (2020). ***b***, Sentinel-1 SAR image of 22 May 2020. Copernicus Sentinel data (2020). ***c***, TerraSAR-X SAR image © DLR. e.V. (2020); Distribution of Airbus DS Geo GmbH. ***d***, COSI SAR image of 27 May 2020 © KARI (2020).

the non-flooded areas were assigned a grid code value of 0 and flooded areas as 1.

Finally, a map was made overlaying base layers such as state, district and block boundaries with infrastructure layers of road, rail and settlements and inundation to prepare a inundation map of the areas affected by cyclone Amphan. The resulting map output was distributed to the concerned state and central government departments for carrying out relief and rescue operations.

Results and discussions

Rainfall during cyclone Amphan between 21 and 26 May 2020 post landfall was monitored using the IMD-GPM merged rainfall daily data[14] (Figure 4).

It was observed that post landfall of the cyclone, intense precipitation was observed during 21–22 May 2020 of the order of 285–300 mm (Figure 4).

Spatial inundation extent

Due to intense precipitation, many areas in the southern part of West Bengal were inundated (Figure 4). Figure 5 shows the sample SAR images acquired over parts of West Bengal.

The pre-cyclone image of Sentinel-1 SAR data (https://peps.cnes.fr/rocket/) was used as the reference image. The inundation in low-lying areas was observed on 22 May 2020. The Terra SAR-X image of 24 May 2020 showed a slight increase in inundation due to heavy rainfall induced by cyclone Amphan on 21 and 23 May 2020. The satellite images acquired during 21, 22, 24, 25 and 27 May 2020 were georeferenced with the master image and water layer was extracted. The water layer was further masked for permanent water bodies and hills, and a final cumulative inundation layer was derived after post editing using GIS analysis. It was observed that more than 209,883 ha spread across ten districts of West Bengal was affected by flood inundation (Figure 6). The inundation is identified by cyan colour. The inundation layer was overlaid on shaded relief DEM of NRSC/ISRO CartoDEM version 3, along with administrative layers and infrastructure layers.

Of the ten districts inundated, East Medinipur was the worst affected with more than 83,402 ha inundated and was mapped almost all the days from 21 to 27 May 2020.

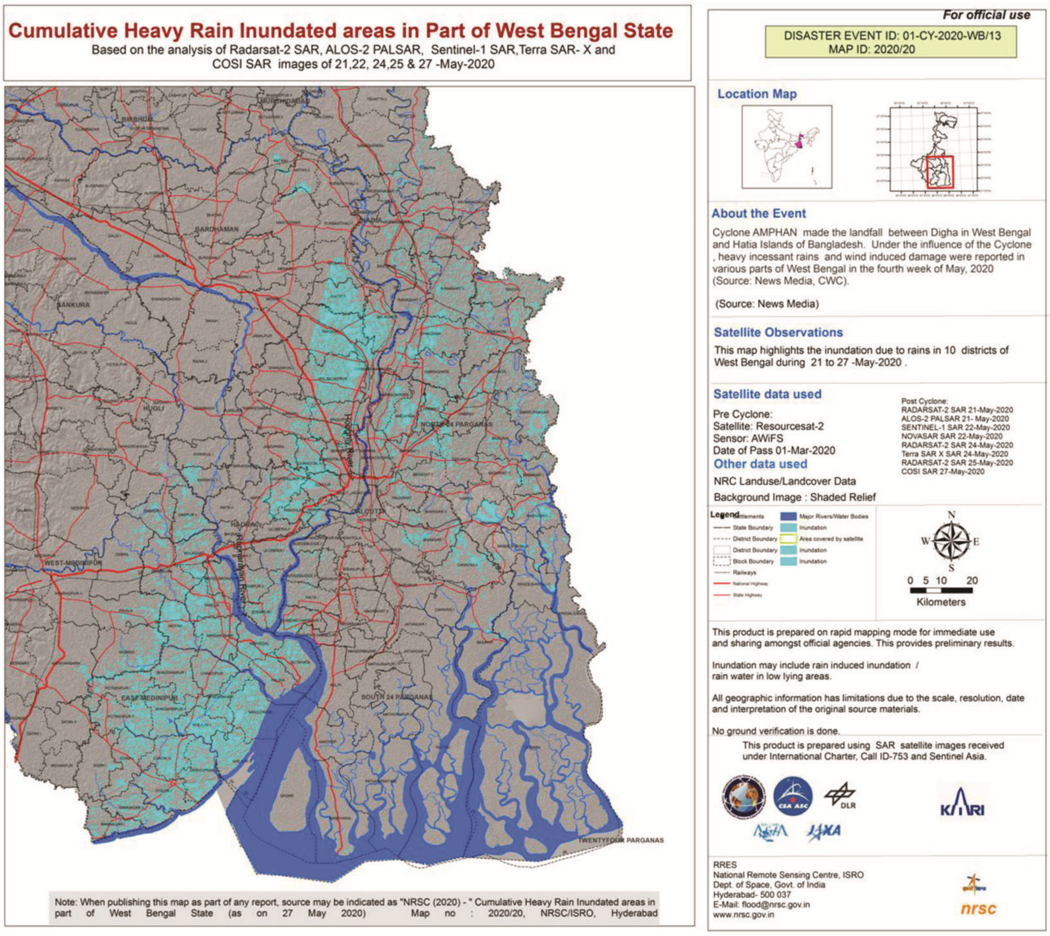

Figure 6. Cumulative inundation map generated for part of West Bengal based on analysis of microwave images of 21–27 May 2020.

Table 2. District-wise inundated area during 21–27 May 2020 in West Bengal, India

District	Inundated area (ha)
East-Medinipur	83,402
Hugli	34,668
North 24 Parganas	33,177
Nadia	17,291
Haora	12,764
West Medinipur	11,593
Bardhaman	8,514
South 24 Parganas	8,129
Murshidabad	185
Kolkata	160
Total	209,883

Figure 5 shows the four SAR images depicting inundation in parts of East Medinipur, Haora and South 24 Paraganas districts. In addition, the districts of Hugli and North 24 Paraganas had an inundation of about 34,668 and 33,177 ha respectively, during the period 21–27 May 2020 (Table 2).

East Medinipur district which is in the southern part of West Bengal, was the worst affected due to cyclone Amphan. Out of more than 80,000 ha which were inundated, many waterlogged areas were also observed. The inundation in low-lying areas was observed using HR data acquired from the International Charter. Figure 7 shows the waterlogged areas in parts of East Medinipur district. The intense precipitation due to cyclone Amphan during 21–25 May 2020 caused the filling up of waterlogged areas across the district. PLEIADES and KOMPSAT3 images acquired on 31 May 2020 show the waterlogged areas in the district. The advantage of availability of cloud-free HR optical data was utilized beneficially to identify the waterlogged areas.

Ground validation

In order to facilitate the ground validation, the inundation layers thus generated from multi-temporal SAR images were transmitted to the WB-RSAC and Disaster Management Department of the Government of West Bengal. The inundation layers were utilized by the State Government to identify the inundated areas and for carrying out relief and rescue measures.

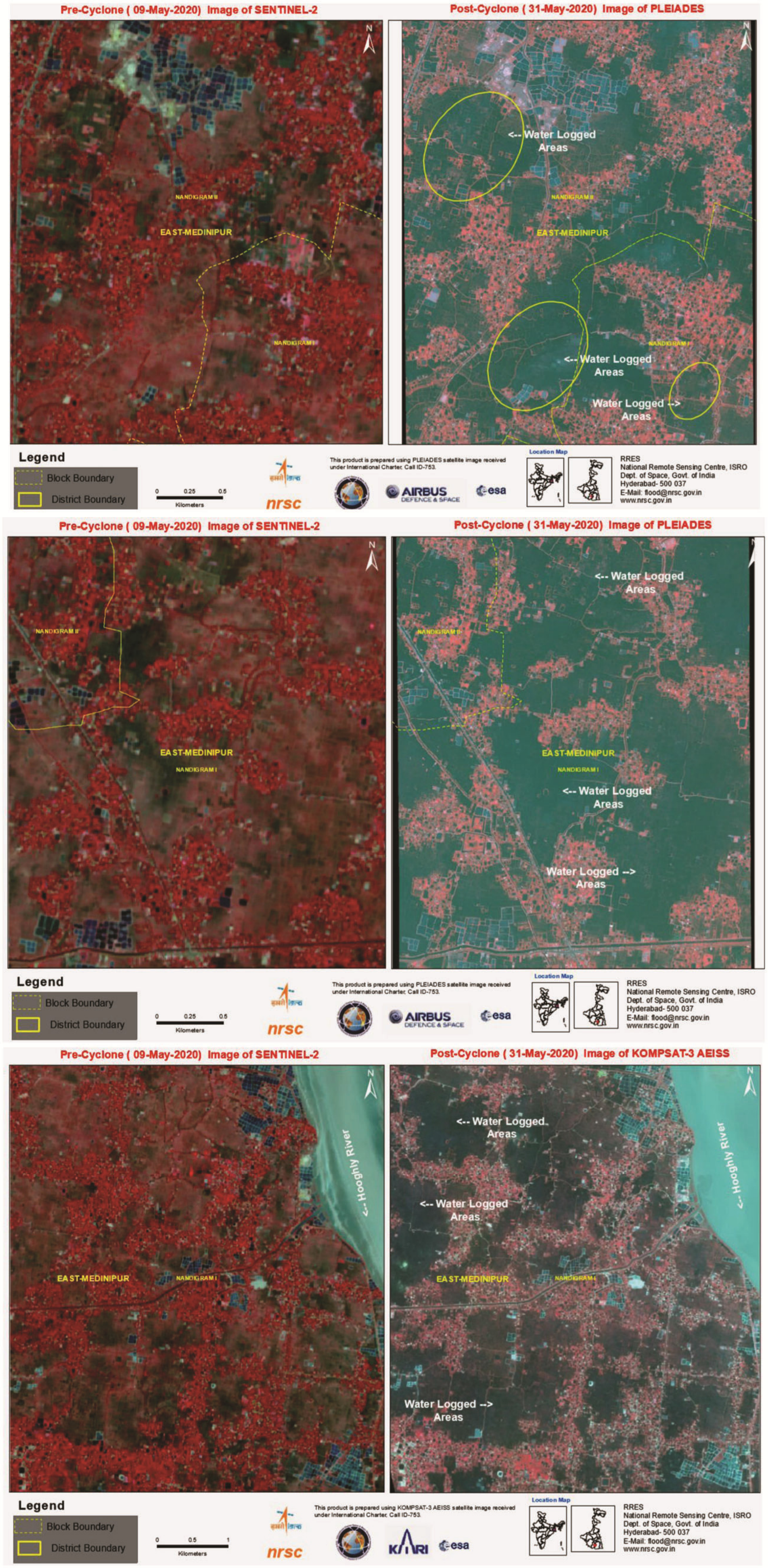

Figure 7. High resolution data showing the waterlogged areas in East Medinipur district, West Bengal.

Conclusion

The present study shows potential operational use of multi-temporal microwave datasets in delineating the cyclone-impacted areas. Inundation maps and VAPs generated using SAR and HR optical data were useful to the central/state disaster management authorities in planning and providing relief and rescue operations on the ground. The study also emphasizes the importance of multiple sources of satellite data in addressing a major cyclonic disaster. The International Charter and SA were helpful in filling up the gaps of satellite constellation in monitoring and mapping of a disaster. In majority of disaster events due to floods, non-availability of satellite data on a daily basis to monitor their progression or recession is a major constraint. To effectively map and monitor them, such as the floods which occur in Assam, Bihar and Odisha, India. These require daily coverage by large swath, multi-frequency medium-resolution SAR data and HR optical data for damage assessment.

1. WMO, Tropical cyclone operational plan for the Bay of Bengal and the Arabian Sea. Tropical Cyclone Programme (TCP) Report No. TCP-21, World Meteorological Organization, 2009 edn, WMO/TD No. 84, 2009.
2. Mohapatra, M. *et al*., Classification of cyclone hazard prone districts of India. *Nat. Hazards*, 2012, **63**, 1601–1620; https://doi.org/10.1007/s11069-011-9891-8.
3. Shultz, J. M., Russell, J. and Espinel, Z., Epidemiology of tropical cyclones: the dynamics of disaster, disease, and development. *Epidemiol. Rev*., 2005, **27**, 21–35.
4. Weinkle, J., Maue, R. and Pielke Jr, R., Historical global tropical cyclone landfalls. *J. Climate*, 2012, **25**, 4729–4735.
5. Hussain, M., Arsalan, M. H., Siddiqi, K., Naseem, B. and Rabab, U., Emerging geo-information technologies (GIT) for natural disaster management in Pakistan: an overview. In Proceedings of the IEEE Second International Conference on Recent Advances in Space Technologies, RAST 2005, 2005, pp. 487–493.
6. Rana, Md S., Gunasekara, K., Hazarika, M. K., Samarakoon, L. and Siddiquee, M., Application of remote sensing and GIS for cyclone disaster management in coastal area: a case study at Barguna district, Bangladesh. *Int. Arch. Photogramm., Remote Sensing Spat. Inf. Sci.*, 2010, **38**(8), 122–126.
7. Wang, F. and Xu, Y. J., Comparison of remote sensing change detection techniques for assessing hurricane damage to forests. *Environ. Monit. Assess*, 2010, **162**, 311–326; doi:10.1007/s10661-009-0798-8.
8. Poompavai, V. and Ramalingam, M., Geospatial analysis for coastal risk assessment to cyclones. *J. Indian Soc. Remote Sensing*, 2013, 1–20.
9. Kaku, K., Satellite remote sensing for disaster management support: a holistic and staged approach based on case studies in Sentinel Asia. *Int. J. Disaster Risk Reduct.*, 2019, **33**, 417–432.
10. Bessis, J.-L., Bequignon, J. and Mahmood, A., The international charter 'space and major disasters' initiative. *Acta Astronaut.*, 2004, **54**(3), 183–190.
11. Xiao, J. F., Li, J. and Moody, A., A detail-preserving and flexible adaptive filter for speckle suppression in SAR imagery. *Int. J. Remote Sensing*, 2003, **24**(12), 2451–2465.
12. Townsend, P. A. and Walsh, S. J., Modelling flood plain inundation using integrated GIS with radar and optical remote sensing. *Geomorphology*, 1998, **21**, 295–312; doi:10.1016/S0169-555X-(97)00069-X.
13. Srinivasulu, J., Sasi Kumar, D., SaiBaba, J. and Prasada Raju, P. V. S. P., Development of a variable threshold method for automatic delineation of flood inundation using RADARSAT SAR data. In Proceedings of the National Workshop on 'Geo-informatics in Water Sector', NWA, IWRS and ISG, Pune, 22–23 September 2005, pp. 115–125.
14. Mitra, A. K., Momin, I. M., Rajagopal, E. N., Basu, S., Rajeevan, M. N. and Krishnamurti, T. N., Gridded daily Indian monsoon rainfall for 14 seasons: merged TRMM and IMD gauge analyzed values. *J. Earth Syst. Sci.*, 2013, **122**(5), 1173–1182.

ACKNOWLEDGEMENTS. We thank the Director, National Remote Sensing Centre (NRSC) and Dr P. V. N. Rao, Deputy Director, Remote Sensing Applications Area, NRSC, Hyderabad for support and guidance while carrying out this work. The study was done under the Disaster Management Support Programme of ISRO. We thank the International Charter and Sentinel Asia for satellite data support.

Received 22 June 2020; revised accepted 12 August 2020

doi: 10.18520/cs/v119/i12/1939-1947